Supplementary Materials for manuscript "**Multidecadal ozone trends in China and implications for human health and crop yields: A hybrid approach combining chemical transport model and machine learning**" authored by Mao et al. (2023)

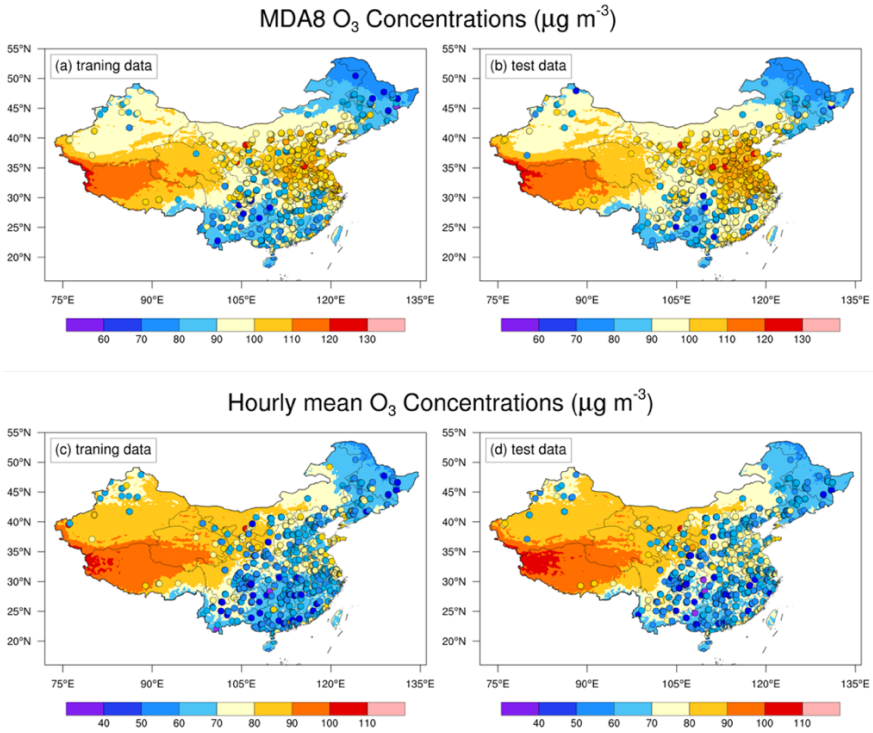

Figure S1. The spatial distribution of O_3 observations (dots) and hybrid model predictions (shaded): (a) MDA8-O_3 concentrations of training data; (b) MDA8-O_3 concentrations of test data; (c) hourly O_3 concentrations of training data; and (d) hourly O_3 concentrations of test data.

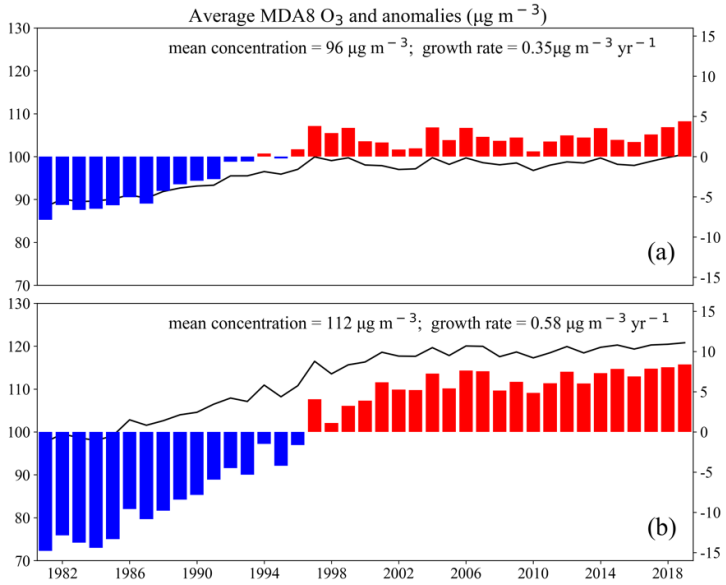

Figure S2. The GEOS-Chem-simulated MDA8-O_3 predictions (black line; left y axis) and corresponding anomalies (colored bar; right y axis) from 1981 to 2019: (a) annual mean; and (b) warm-season mean (May-September). Observed trends (growth rate) are obtained by ordinary linear regression on mean values of MDA8-O_3. The anomalies are defined as annual mean minus the multi-decadal average over 1981-2019.

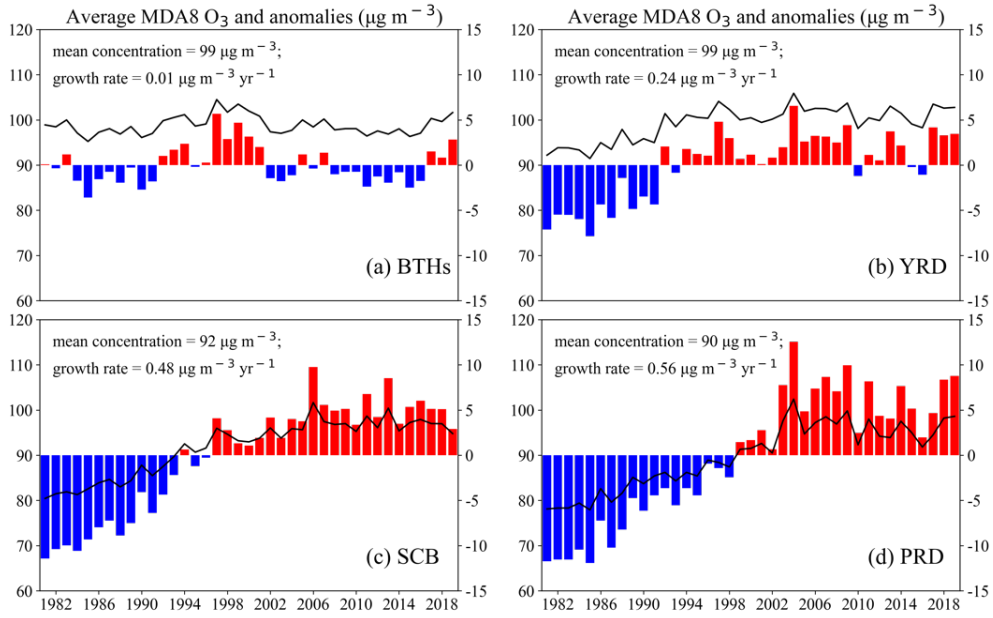

Figure S3. The annual averaged MDA8 O_3 concentrations of bias-corrected predictions (black line; left y axis) and corresponding anomalies (colored bar; right y axis) from 1981 to 2019: (a) BTHs; (b) YRD; (c) SCB; and (d) PRD. Observed trends (growth rate) are obtained by ordinary linear regression on mean values of MDA8 O_3.

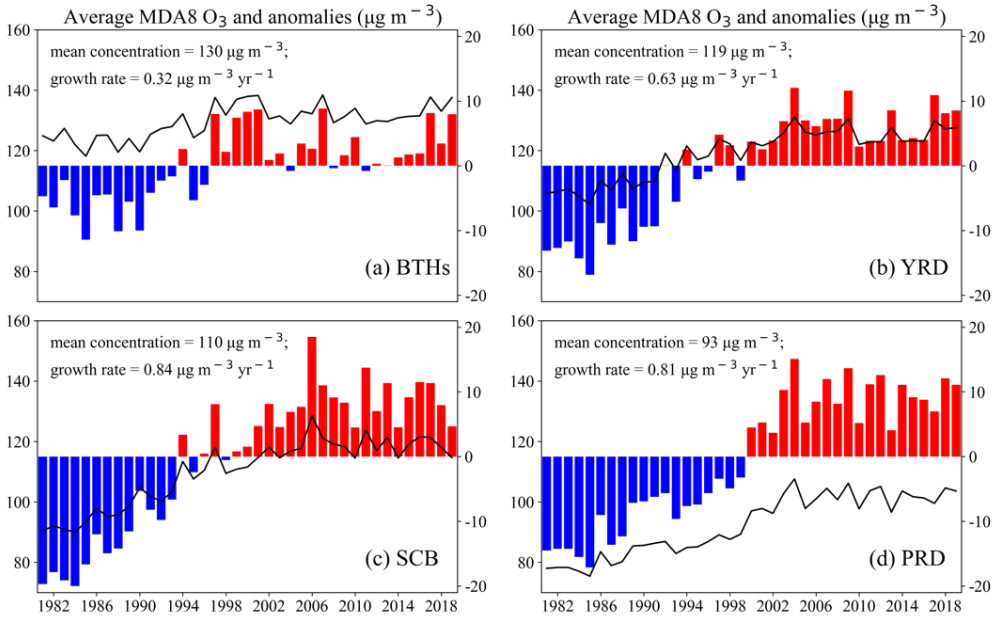

Figure S4. The same as Figure S3, but for warm-season averaged MDA8 O_3 concentrations.

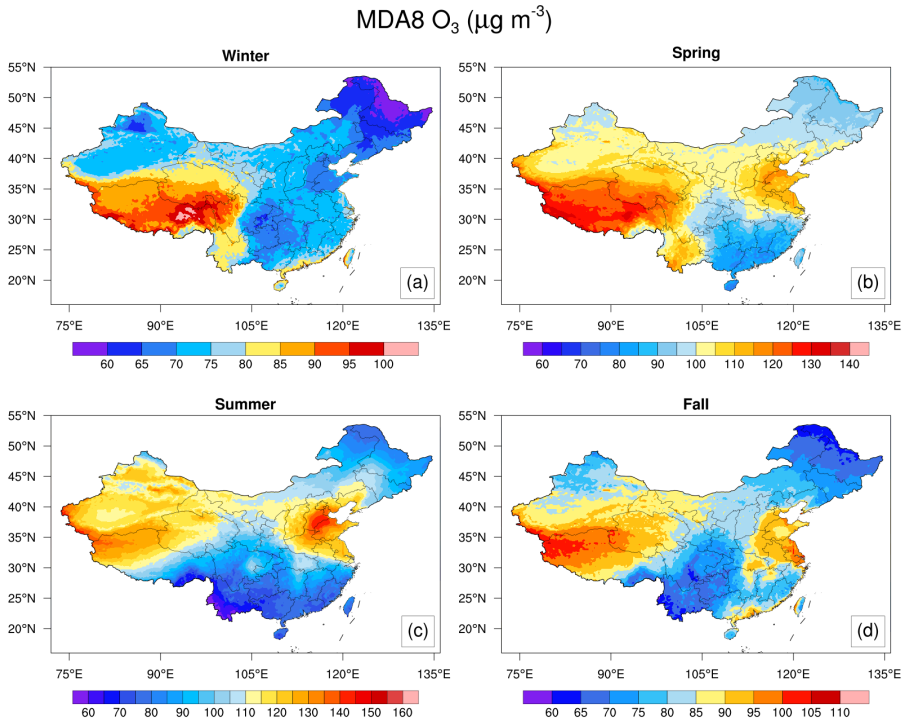

Figure S5. Spatial distribution of the bias-corrected MDA8-O_3 predictions (μg m^{-3}) from 1981–1990: (a) winter; (b) spring; (c) summer; and (d) fall.

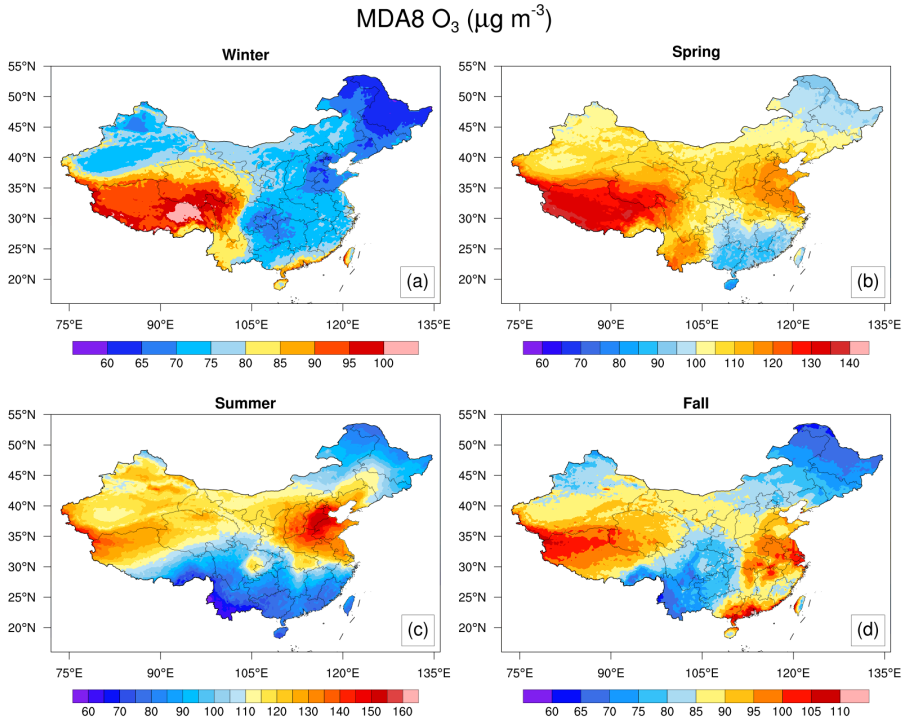

Figure S6. Same as Fig. S6 but for the period of 1991–2000.

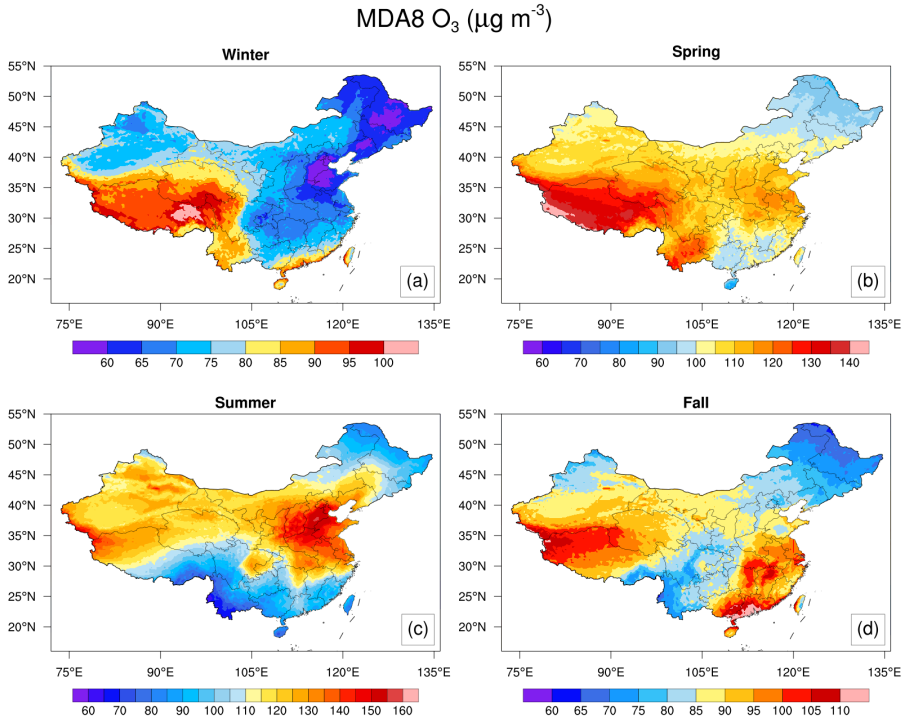

Figure S7. Same as Fig. S6 but for the period of 2001–2010.

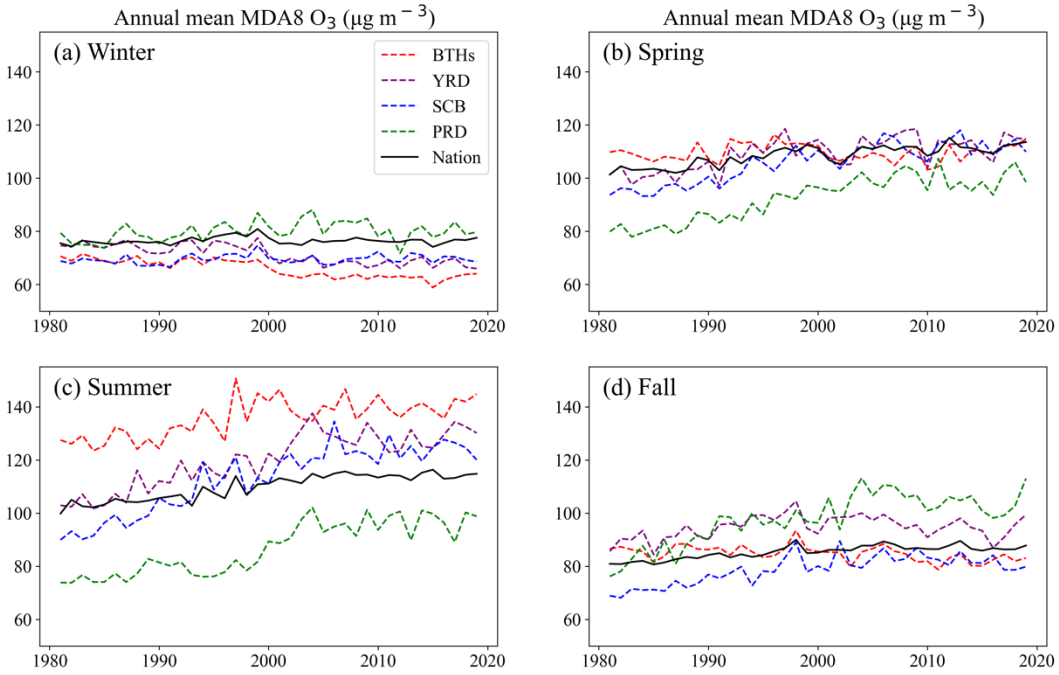

Figure S8. The seasonal averaged bias-corrected MDA8-O_3 concentrations in different regions from 1981 to 2019: (a) winter; (b) spring; (c) summer; and (d) fall.

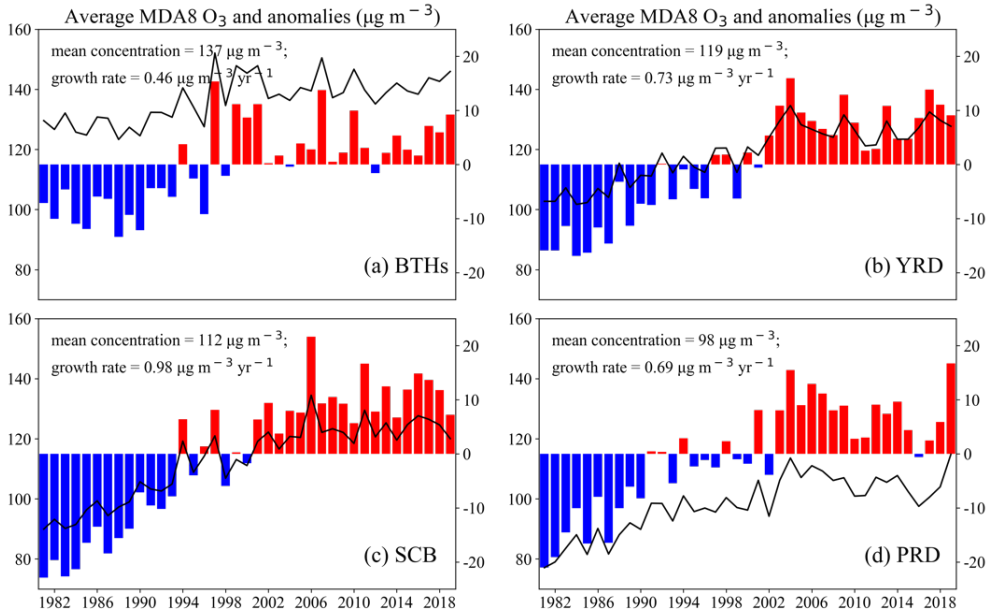

Figure S9. The same as Figure S3, but for summer averaged MDA8 O_3 concentrations in BTHs, YRD and SCB, and fall averaged MDA8 O_3 concentrations in PRD.

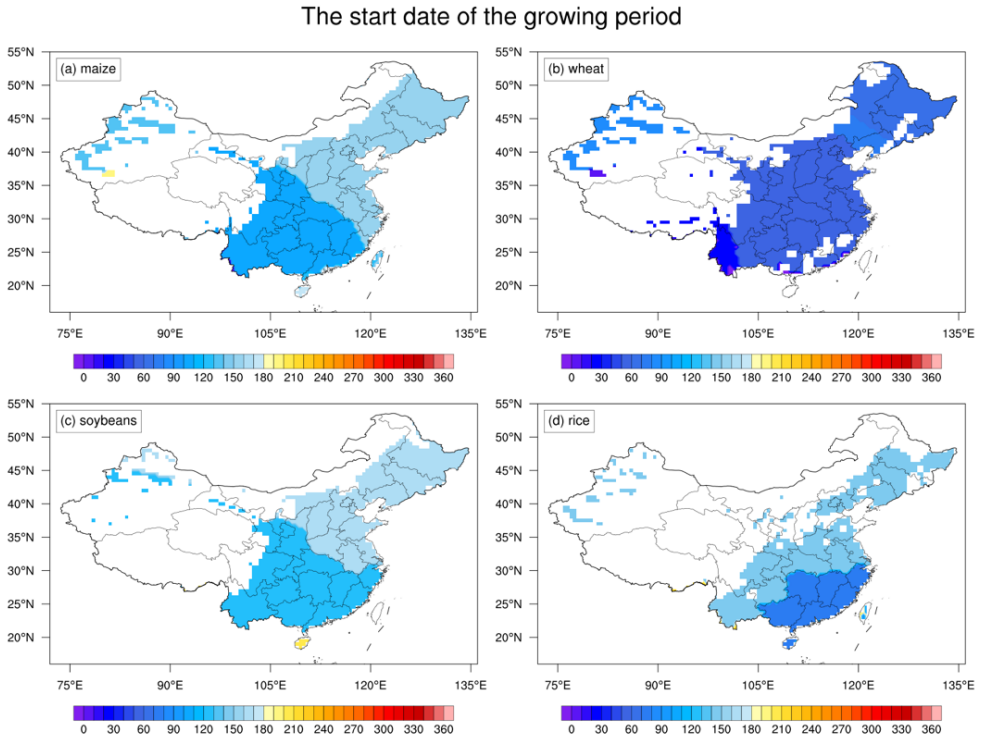

Figure S10. The start of the growing period for crops: (a) maize; (b) wheat; (c) soybean; and (d) rice. The growing period are defined as the 90 days prior to the start of the harvesting period according to the crop calendar.

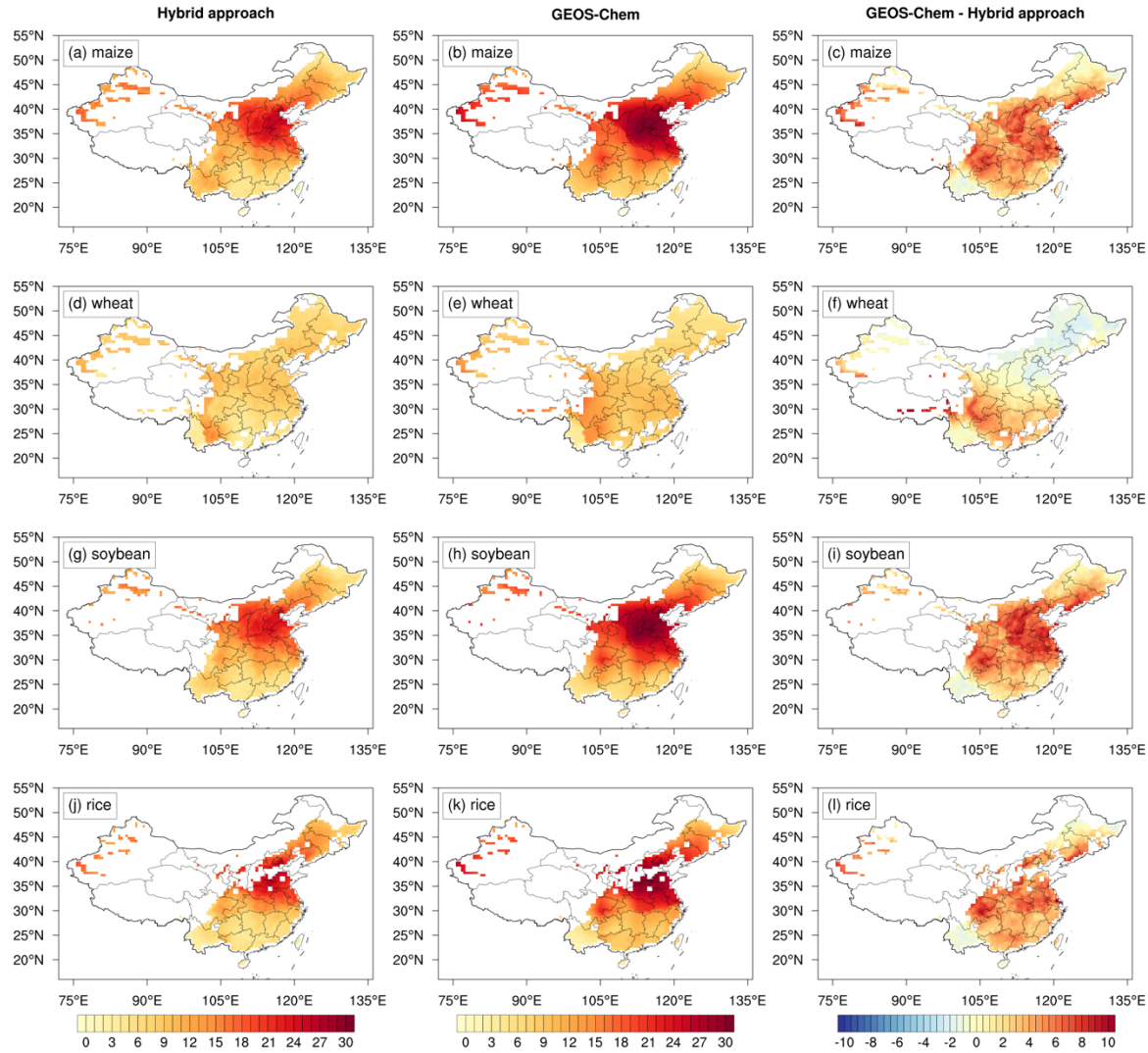

Figure S11. Spatial distribution of annual average AOT40 for four staple crops during the growing season. The estimated AOT40 using bias-corrected O_3: (a) maize; (d) wheat; (g) soybean; and (j) rice. The estimated AOT40 using GEOS-Chem-simulated O_3: (b) maize; (e) wheat; (h) soybean; and (k) rice. The differences in estimated AOT40 between GEOS-Chem-simulated and bias-corrected O_3: (c) maize; (f) wheat; (i) soybean; and (l) rice. The GEOS-Chem-simulated O_3 were regridded to 0.5°×0.5° for comparison with bias-corrected O_3.

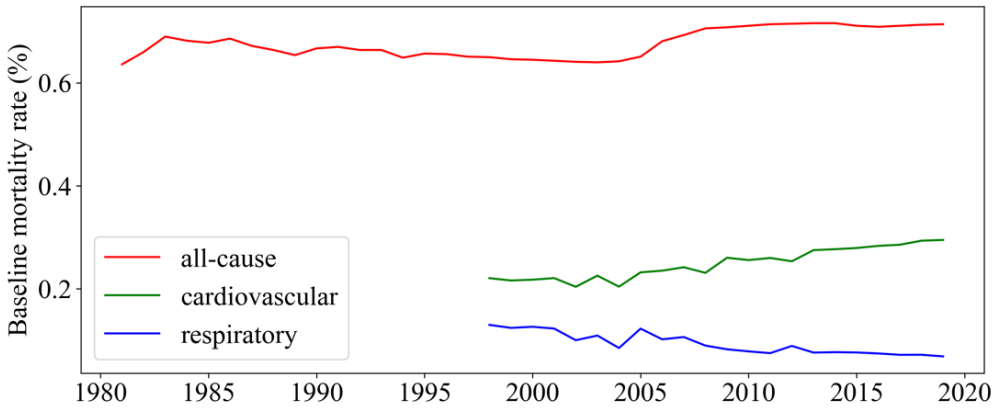

Figure S12. Annual baseline mortality rate (%) for particular disease: (a) all-cause disease; (b) cardiovascular disease; and (c) respiratory disease.

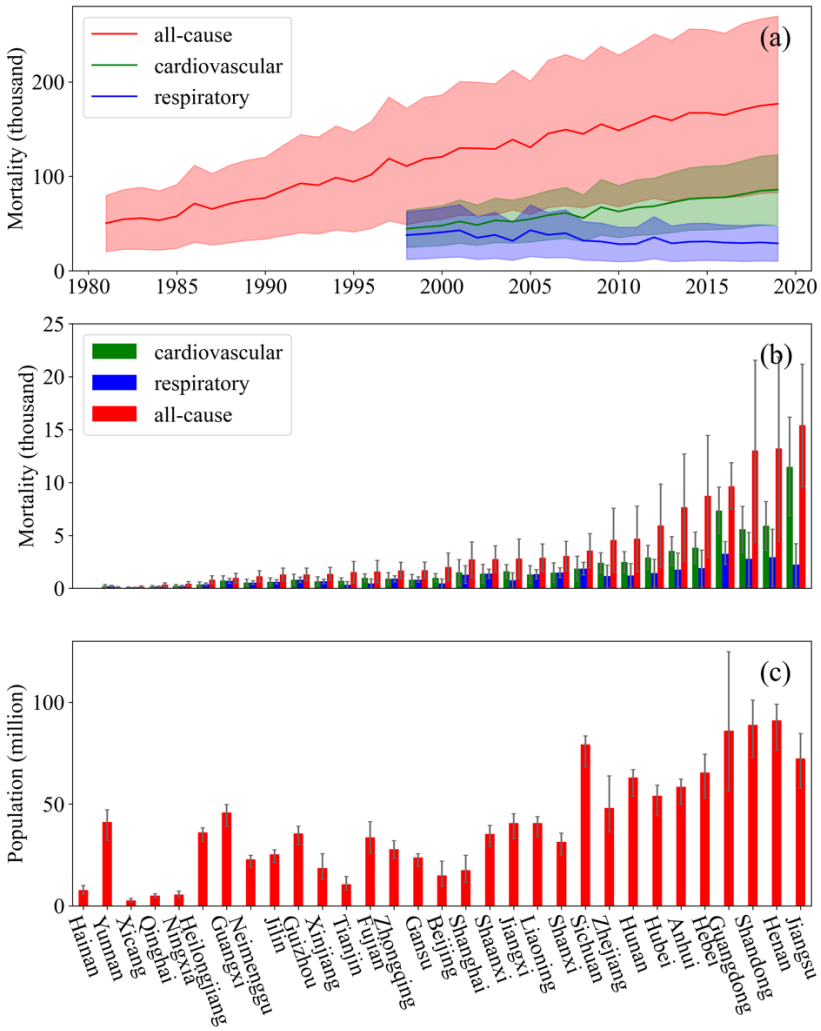

Figure S13. (a) Annual premature morality (thousand) for different diseases over the past decades; (b) annual mean province-based morality (thousand) attributed to different health endpoints; and (c) annual mean province-based population (million). The morality is calculated using the GEOS-Chem-simulated O_3.

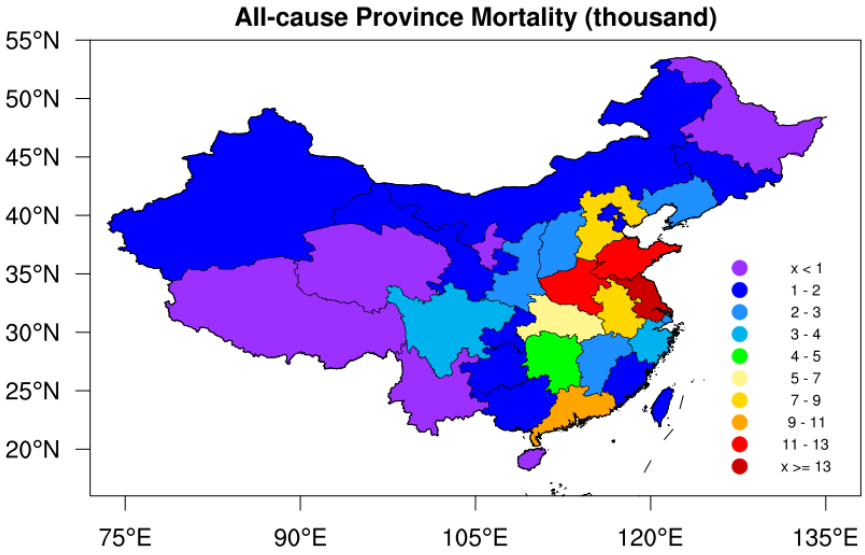

Figure S14. Provincial annual premature morality (thousand) for all-cause diseases from 1981 to 2019.

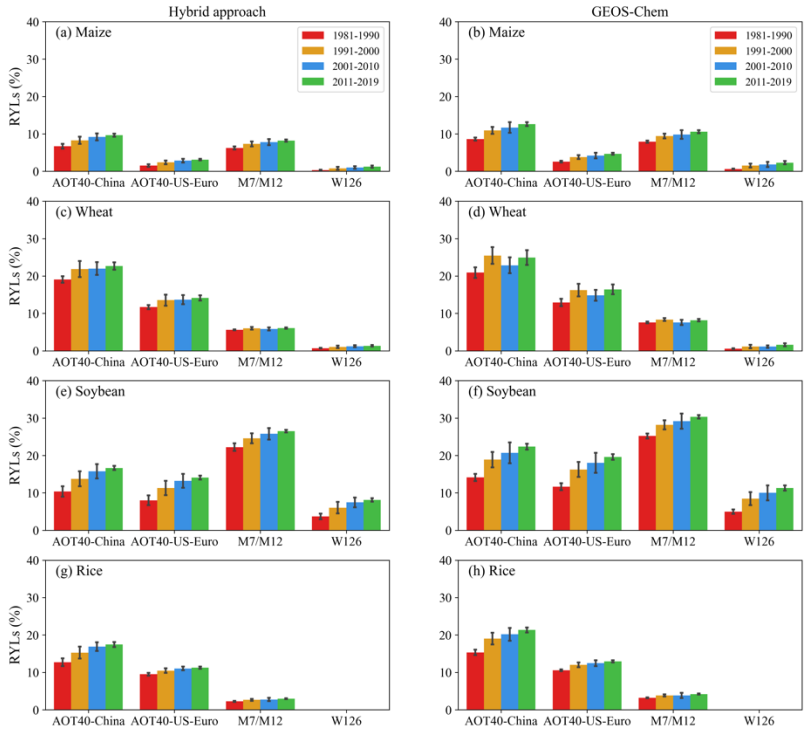

Figure S15. The estimated decadal mean relative yield losses (RYLs) of four staple crops using different metrics and dose-yield relationships from 1981–2019. The estimated RYLs using bias-corrected O_3: (a) maize; (c) wheat; (e) soybean; and (g) rice. The estimated RYLs using GEOS-Chem-simulated O_3: (b) maize; (d) wheat; (f) soybean; and (h) rice. The error bar represents the standard deviation. The dose-yield relationships of AOT40-US-Euro for four crops are derived from (Mills et al., 2007), M7 for rice and wheat are from (Adams et al., 1989), M12 for soybean and maize are from (Lesser et al., 1990), and W126 for maize, wheat and soybean are from (Tai et al., 2021), respectively.

Table S1 The information of the candidate variables used for training.

Symbols	Units	Description	Source
GEOS_O_3	ppb	GEOS-Chem-simulated O_3	GEOS-Chem output
Lat	°	Latitude of site/grid	
Lon	°	Longitude of site/grid	
Hourly_ O_3	μg m^{-3}	Hourly mean O_3 concentration	Calculated from GEOS_O_3
Monthly_ O_3	μg m^{-3}	Monthly mean O_3 concentration	Calculated from GEOS_O_3
Albedo		Surface albedo	ERA5
SSRD	J m^{-2}	Downward surface solar radiation	ERA5
SP	Pa	Surface pressure	ERA5
T2M	K	Air temperature at 2m	ERA5
RH_1000hPa	%	Relative humidity at 1000 hPa	ERA5
RH_850hPa	%	Relative humidity at 850 hPa	ERA5
U10	m s^{-1}	U component of wind at 10 m	ERA5
V10	m s^{-1}	V component of wind at 10 m	ERA5
U_1000hPa	m s^{-1}	U component of wind at 1000 hPa	ERA5
V_1000hPa	m s^{-1}	U component of wind at 1000 hPa	ERA5
U_850hPa	m s^{-1}	V component of wind at 850 hPa	ERA5
V_850hPa	m s^{-1}	V component of wind at 850 hPa	ERA5
Omega_1000hPa	Pa s^{-1}	Vertical velocity at 1000 hPa	ERA5
Omega _850hPa	Pa s^{-1}	Vertical velocity at 850 hPa	ERA5
Elevation	m	Elevation of site/grid	RESDC
LU		Land use type of site/grid	RESDC

Table S2 Statistical relationships between relative yields (RYs) and AOT40. RY is defined as the ratio of O_3-affected yield to the unaffected yield at zero O_3 exposure.

Crop	Dose-yield relationship	References
Maize	$RY = 1 – S[AOT40 + (40 – x) * 1.08 – (20.22 –0.01264x^2) / (1 + 0.207\ AOT40 – 0.0001293x^2\ AOT40)] / [1 – S\ (22.98 – 1.08x + 0.01264x^2)]$, $S = 0.0068$ and $x = 40.0$	(Feng et al., 2022)
Wheat	$RY = 1 – S[AOT40 + (40 – x) * 1.08 – (20.22 –0.01264x^2) / (1 + 0.207\ AOT40 – 0.0001293x^2\ AOT40)] / [1 – S\ (22.98 – 1.08x + 0.01264x^2)]$, $S = 0.0161$ and $x = 26.5$	(Feng et al., 2022)
Soybean	$RY = 1 – 0.012AOT40$	(Zhang et al., 2017)
Rice	$RY = 1 – S[AOT40 + (40 – x) * 1.08 – (20.22 –0.01264x^2) / (1 + 0.207\ AOT40 – 0.0001293x^2\ AOT40)] / [1 – S\ (22.98 – 1.08x + 0.01264x^2)]$, $S = 0.0071$ and $x = 19.4$	(Feng et al., 2022)

Table S3 Seasonal averaged MDA8 O_3 concentrations (μg m^{-3}) in each region from 1981 to 2019. The differences are GEOS-Chem minus Hybrid approach.

Seasons	Region	Hybrid approach	GEOS-Chem	Differences
Winter	BTHs	65 ± 4	63 ± 7	-2 ± 3
	YRD	73 ± 3	72 ± 7	-2 ± 4
	SCB	69 ± 2	79 ± 2	10 ± 1
	PRD	81 ± 4	87 ± 3	6 ± 2
	Nation	73 ± 2	76 ± 3	3 ± 2
Spring	BTHs	109 ± 3	102 ± 4	-7 ± 3
	YRD	109 ± 6	110 ± 5	1 ± 3
	SCB	106 ± 7	112 ± 8	7 ± 2
	PRD	93 ± 9	93 ± 11	6 ± 3
	Nation	106 ± 4	105 ± 4	-1 ± 1
Summer	BTHs	137 ± 8	142 ± 7	5 ± 2
	YRD	119 ± 10	125 ± 11	6 ± 4
	SCB	113 ± 12	120 ± 14	7 ± 3
	PRD	88 ± 10	87 ± 15	-1 ± 5
	Nation	111 ± 7	114 ± 9	3 ± 2
Fall	BTHs	83 ± 3	83 ± 5	-1 ± 2
	YRD	95 ± 4	103 ± 3	6 ± 2
	SCB	79 ± 5	95 ± 7	17 ± 3
	PRD	98 ± 10	101 ± 12	3 ± 4
	Nation	86 ± 3	92 ±4	6 ± 1

Table S4 Exposure-response coefficients for the short-term health impacts of O_3.

Health outcomes	Coefficients β	95% CI	Study region/year	Referenced paper
All-cause	4.5E–04	1.6E–04 – 7.3E–04	Shanghai (2001–04)	(Zhang et al., 2006)
	5.5E–04	3.4E–04 – 7.6E–04	Jiangsu (2013–14)	(Chen et al., 2017)
	8.1E–04	6.3E–04 – 1.00E–03	PRD (2006–08)	(Tao et al., 2011)
	3.6E–04	1.2E–04 – 6.0E–04	East China (2005–30)	(Madaniyazi et al., 2016)
	2.4E–04	1.3E–04 – 3.5E–04	Nationwide (2013–15)	(Yin et al., 2017)
Cardiovascular	5.3E–04	1.0E–04 – 9.6E–04	Shanghai (2001–04)	(Zhang et al., 2006)
	9.8E–04	5.8E–04 – 1.4E–03	Jiangsu (2013–14)	(Chen et al., 2017)
	1.01E–03	7.1E–04 – 1.32E–03	PRD (2006–08)	(Tao et al., 2011)
	3.8E–04	2.3E–04 – 5.3E–04	East China (2005–30)	(Madaniyazi et al., 2016)
	2.7E–04	1.0E–04 – 4.4E–04	Nationwide (2013–15)	(Yin et al., 2017)
Respiratory	3.5E–04	–4.0E–04 – 1.09E–03	Shanghai (2001–04)	(Zhang et al., 2006)
	1.3E–03	8.9E–04 – 1.76E–03	PRD (2006–08)	(Tao et al., 2011)
	5.1E–04	3.0E–05 – 9.8E–04	East China (2005–30)	(Madaniyazi et al., 2016)
	7.3E–04	4.9E–04 – 9.7E–04	Nationwide	(Shang et al., 2013)

References

Adams, R. M., Glyer, J. D., Johnson, S. L., and McCarl, B. A.: A Reassessment of the Economic Effects of Ozone on U.S. Agriculture, JAPCA, 39, 960-968, https://doi.org/10.1080/08940630.1989.10466583, 1989.

Chen, K., Zhou, L., Chen, X., Bi, J., and Kinney, P. L.: Acute effect of ozone exposure on daily mortality in seven cities of Jiangsu Province, China: No clear evidence for threshold, Environmental Research, 155, 235-241, https://doi.org/10.1016/j.envres.2017.02.009, 2017.

Feng, Z., Xu, Y., Kobayashi, K., Dai, L., Zhang, T., Agathokleous, E., Calatayud, V., Paoletti, E., Mukherjee, A., Agrawal, M., Park, R. J., Oak, Y. J., and Yue, X.: Ozone pollution threatens the production of major staple crops in East Asia, Nature Food, 3, 47-56, https://doi.org/10.1038/s43016-021-00422-6, 2022.

Lesser, V. M., Rawlings, J. O., Spruill, S. E., and Somerville, M. C.: Ozone Effects on Agricultural Crops: Statistical Methodologies and Estimated Dose-Response Relationships, Crop Science, 30, cropsci1990.0011183X003000010033x, https://doi.org/10.2135/cropsci1990.0011183X003000010033x, 1990.

Madaniyazi, L., Nagashima, T., Guo, Y., Pan, X., and Tong, S.: Projecting ozone-related mortality in East China, Environment International, 92-93, 165-172, https://doi.org/10.1016/j.envint.2016.03.040, 2016.

Mills, G., Buse, A., Gimeno, B., Bermejo, V., Holland, M., Emberson, L., and Pleijel, H.: A synthesis of AOT40-based response functions and critical levels of ozone for agricultural and horticultural crops, Atmospheric Environment, 41, 2630-2643, https://doi.org/10.1016/j.atmosenv.2006.11.016, 2007.

Shang, Y., Sun, Z., Cao, J., Wang, X., Zhong, L., Bi, X., Li, H., Liu, W., Zhu, T., and Huang, W.: Systematic review of Chinese studies of short-term exposure to air pollution and daily mortality, Environment International, 54, 100-111, https://doi.org/10.1016/j.envint.2013.01.010, 2013.

Tai, A. P. K., Sadiq, M., Pang, J. Y. S., Yung, D. H. Y., and Feng, Z.: Impacts of Surface Ozone Pollution on Global Crop Yields: Comparing Different Ozone Exposure Metrics and Incorporating Co-effects of CO2, Frontiers in Sustainable Food Systems, 5, https://doi.org/10.3389/fsufs.2021.534616, 2021.

Tao, Y., Zhong, L., Huang, X., Lu, S.-E., Li, Y., Dai, L., Zhang, Y., Zhu, T., and Huang, W.: Acute mortality effects of carbon monoxide in the Pearl River Delta of China, Science of The Total Environment, 410-411, 34-40, https://doi.org/10.1016/j.scitotenv.2011.09.004, 2011.

Yin, P., Chen, R., Wang, L., Meng, X., Liu, C., Niu, Y., Lin, Z., Liu, Y., Liu, J., Qi, J., You, J., Zhou, M., and Kan, H.: Ambient Ozone Pollution and Daily Mortality: A Nationwide Study in 272 Chinese Cities, Environ Health Perspect, 125, 117006, https://doi.org/10.1289/EHP1849, 2017.

Zhang, W., Feng, Z., Wang, X., Liu, X., and Hu, E.: Quantification of ozone exposure- and stomatal uptake-yield response relationships for soybean in Northeast China, Science of The Total Environment, 599-600, 710-720, https://doi.org/10.1016/j.scitotenv.2017.04.231, 2017.

Zhang, Y., Huang, W., London Stephanie, J., Song, G., Chen, G., Jiang, L., Zhao, N., Chen, B., and Kan, H.: Ozone and Daily Mortality in Shanghai, China, Environmental Health Perspectives, 114, 1227-1232, https://doi.org/10.1289/ehp.9014, 2006.